ACS APPLIED MATERIALS & INTERFACES

Research Article

www.acsami.org

Nanoporous Membranes with Tunable Pore Size by Pressing/Sintering Silica Colloidal Spheres

Amir Khabibullin and Ilya Zharov*

Department of Chemistry, University of Utah, 315 South 1400 East, Salt Lake City, Utah 84112, United States

ABSTRACT: We prepared robust nanoporous membranes with controlled area and uniform thickness by pressing silica colloidal spheres into disks followed by sintering. Three different diameters of silica particles, 390, 220, and 70 nm, were used to prepare the membranes with different pore size. In order to evaluate their size-selectivity, we measured the diffusion of polystyrene particles through these membranes. Although pressed silica colloidal membranes do not possess visible order or uniform pore size, they showed size-selective transport. We also demonstrated that pressed silica colloidal membranes can be functionalized via pore-filling. Sulfonated polymer brushes were grown inside the pores via surface-initiated atom transfer radical polymerization, which resulted in a material with high proton conductivity suitable for fuel cell applications.

KEYWORDS: *nanoporous membranes, silica colloidal spheres, size-selective diffusion, pore-filled membranes*

INTRODUCTION

Over the past decade, nanoporous membranes attracted increasing attention due to their potential applications in molecular sorting, separations, and sensing.[1−3] Several methods have been developed for the preparation of nanoporous membranes including lithography,[4] anodization of aluminum,[5] track etching of polymers,[6] surfactant-directed self-assembly,[7] self-assembly of block copolymers,[8] self-assembly and polymerization of liquid crystals,[9−11] sol−gel methods,[12,13] dip-coating,[14] chemical vapor deposition,[15] and by templating silica colloidal crystals.[16,17]

For any emerging membrane technology to be commercially successful requires both the ability to scale up the membrane preparation process and the ability to control the average pore diameter with a narrow pore diameter distribution to enable size exclusion separations. Presently, depending on the membrane material the pore size is controlled by preparation conditions, such as etching conditions in ion-track membranes and anodized alumina membranes, or predetermined by the size of the template used in membrane preparation.[16,17]

Inorganic membranes[18] are particularly attractive in the fields of high temperature gas separation,[19,20] water treatment,[21] and as catalytic support and membrane reactors[22] due to their mechanical, chemical and thermal stability. Most commonly, inorganic nanoporous membranes are prepared by anodization of aluminum[5] and by sol−gel methods.[12] These methods, however, are not very time- and cost-effective.

Assembly of silica colloidal spheres provides an alternative attractive approach to the preparation of inorganic nanoporous membranes with high thermal and chemical stability. Colloidal spheres self-assemble into silica colloidal crystals in which the spheres are arranged in close-packed face-centered cubic (fcc) packing. This arrangement inherently includes ordered interconnected three-dimensional voids, accessible for molecular transport.[23] The void size in colloidal crystals varies in the wide range (5−100 nm) depending on the silica sphere diameter.[23] Earlier, we reported[24] the preparation of mechanically stable and mechanical defect-free colloidal membranes with approximately 1 × 1 cm × 200 μm dimensions by sintering ordered silica colloidal crystals at 1050 °C. We also demonstrated[25] that molecular transport through these membranes is characterized by high size-selectivity, which is enhanced by the tortuosity of the diffusion pathway in the colloidal crystal. Our results suggested that sintered silica colloidal membranes have potential applications in size-selective separations. In addition, we showed that surface modification of colloidal nanopores leads to gated silica colloidal membranes.[26]

However, ordered silica colloidal crystals used in the preparation of the above membranes are limited in size, which results in small area of the corresponding membranes. It is also difficult to obtain silica colloidal crystals of uniform thickness by vertical deposition from colloidal suspensions, yet uniform thickness is important for practical applications of nanoporous membranes.[27]

To further improve the preparation of silica colloidal membranes, we decided to prepare these membranes by pressing silica spheres together in a die set. This would provide uniform membrane thickness, while the membrane area would be limited only by the die set dimensions. This process would be time-efficient compared to the vertical deposition, which requires hours. Surprisingly, despite these attractive features, to the best of our knowledge such a method has not been described before. On the other hand, the resulting colloidal

Received: February 17, 2014
Accepted: April 21, 2014
Published: April 21, 2014

   dx.doi.org/10.1021/am501002z | ACS Appl. Mater. Interfaces 2014, 6, 7712−7718

membranes would possess no crystalline order, thus not containing uniform pores and requiring verification of size exclusion behavior.

In this article, we report the preparation of nanoporous membranes by pressing silica spheres with a hydraulic press at 5000 lb followed by sintering at 1050 °C. We studied the diffusion of a dye-labeled dendrimer and of polystyrene nanospheres of various diameters through pressed silica colloidal membranes to determine the "cut-off" of the membranes and to demonstrate its tunability. We also performed pore-filling of these membranes with a proton conducting polymer.

MATERIALS AND METHODS

Materials and Instruments. Ammonium hydroxide (28−30% as NH_3, EMD Chemicals, Inc.), tetraethyl orthosilicate (99.999% metal basis, Alfa Aesar), Polyspherex Polystyrene spheres of 25 nm, 100 nm, and 250 nm diameter (Phosphorex Inc.), and 3-sulfopropyl methacrylate (Aldrich) were used as received. Deionized water with 18 MΩ resistivity used in all experiments was obtained from a Barnstead "E-pure" water purification system. All ethanol used was 200 proof. Scanning electron microscopy (SEM) images were obtained using a FEI Novanano 630 instrument. Optic microscopy images were obtained using a Nikon Eclipse ME600 instrument. A Branson 1510 sonicator was used for all sonications. UV/vis measurements were performed using an Ocean Optics USB2000 or USB4000 instrument. A Clay Adams Compact II Centrifuge (3200 rpm, Becton Dickinson) was used for all centrifugations. A Fisher Scientific Isotemp Programmable Muffle Furnace (Model 650) was used for calcination and sintering.

Preparation of Silica Spheres. Silica spheres were prepared from tetraethoxysilane (TEOS) in ethanol in the presence of water and ammonia according to the previously reported procedure.[24,28] For the preparation of 390 nm silica spheres the final concentrations in reaction mixture were 0.2 M TEOS, 1.1 M NH_3, and 17.0 M H_2O. After repeated washing using ethanol and water, the silica spheres were dried in a stream of nitrogen. The dried spheres were then calcinated for 4 h at 600 °C. SEM images of the spheres were obtained, and the diameters were determined from 100 individually measured silica spheres in each sample to be 390 ± 10 nm after the calcination.

Silica spheres of 220 nm diameter were prepared following the same procedure but using different amounts of reagents. The final concentrations of the reagents were 0.2 M TEOS (51.4 mL, 0.20 mol), 0.4 M NH_3 (26.78 mL, 0.4 mol), and 16.0 M H_2O (288 g, 16.0 mol). SEM images of the spheres were obtained, and the diameters were determined from 100 individually measured silica spheres in each sample to be 260 ± 20 nm and 230 ± 20 nm before and after calcination, respectively.

Silica spheres of 70 nm in diameter were prepared and calcinated following the reported procedure.[29] The following concentrations of the reagents were used: TEOS (15.2 mL, 0.12 M final concentration) and NH_4OH (24.2 mL, 0.80 M NH_4OH final concentration). SEM images of the spheres were obtained, and the diameter was determined from 100 individually measured silica spheres to be 70 ± 10 nm after the calcination.

Preparation of Pressed Silica Colloidal Membranes. A stainless steel dry pressing die set (13 mm ID, supplied by iCL, Inc.) was loaded with dry silica spheres (all large aggregates were broken using spatula) and placed in a Carver laboratory hydraulic press. A pressure of 5000 pounds was applied for 30 s, after which the pressed material was carefully removed from the die set and placed into the oven, covered with a small ceramic plate to create even distribution of heat and prevent curving, and heated at 1050 °C for 12 h. The membrane shrunk to 10.5 mm in diameter after the sintering. The thickness of the membrane could be varied from 0.9 to 1.5 mm by the amount of silica spheres used. The thickness was measured with digital calipers. Silica membranes of 30 mm diameter were prepared following the same procedure and using a 30 mm ID stainless steel dry pressing die set (Across International, NJ). Upon sintering at 1050 °C for 24 h the diameter of the pressed membranes decreased to 25 mm. The photographs of silica colloidal membranes are shown in Figure 2.

Mechanical Testing of Pressed Silica Colloidal Membranes. We used the four-point bending test to determine the flexural strength of the membranes. This test uses a rectangular beam of the analyzed material supported at two points from below (the support span) and bearing a load that makes contact at two points above (the loading span). The load is increased until the beam fractures, and this rupture force is used to calculate the flexural strength. If the loading span is one-third of the length of the support span, then the flexural strength is calculated as $\sigma = (FL/bd^2)$, where σ is flexural strength (Pa), F is rupture force (N), L is support length (m), b is beam width (m), and d is beam thickness (m). A test apparatus was constructed with 4 cm in its largest dimension (Figure 1). Copper rods 1 mm in diameter were used to form the contact points of the loading and support spans and were mounted on acrylic sheets. The apparatus consisted of two pieces: a base containing the supporting rods and a top containing the load contact points. The base also had rods inserted vertically into the corners that aligned with holes in the top piece. We used a hanging weight that was attached to the two ends of the beam that rested across the top of the apparatus to apply pressure to the membrane samples. The membrane test samples were cut to a rectangular shape using a carbon dioxide laser.

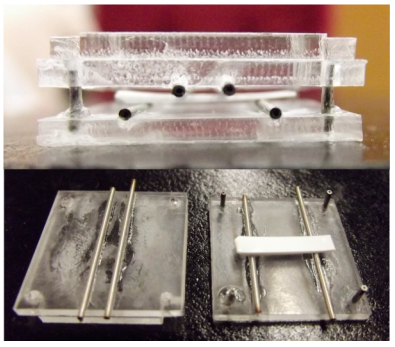

Figure 1. 4-Point bending test apparatus assembled (top) and disassembled (bottom).

Diffusion Measurements. Diffusion of the dendrimer and polystyrene beads of different diameters through the colloidal membranes was measured spectrophotometrically according to the previously reported procedure.[25] The concentration of the PS beads in the feed cuvette was ca. 10^{13} particles/mL for each PS size. The flux of PS beads was measured by recording the absorbance at 546 nm for dye-labeled dendrimers and at 250 nm for polystyrene spheres. To use a membrane in a new experiment, it was soaked in deionized water for 2 days, with fresh water being used several times to remove any remaining dendrimer or PS beads from the membrane.

Pore-Filling of Pressed Silica Colloidal Membranes. Pore-filling with proton conducting polymer brushes was carried out according to previously reported procedure[30] via surface-initiated ATRP. Sintered colloidal membranes were first modified with ATRP initiator 2-bromoisobutyryl bromide, followed by the polymerization of the monomer, poly(3-sulfopropyl methacrylate) inside the initiator-modified silica membranes via ATRP at room temperature for 12 h. A representative SEM image of the pore-filled silica colloidal membrane is shown in Figure 5.

Proton Conductivity Measurements. Proton conductivity of the pore-filled silica colloidal membranes was measured using electrochemical impedance spectroscopy. The impedance was measured at room temperature according to the previously reported procedure.[30] The relative humidity was kept at 98% during the experiments. The complex impedance of the samples was measured and the proton conductivity was calculated using $\sigma = l/RA$, where σ is the ionic conductivity, l is the distance between the two electrodes, R is the

dx.doi.org/10.1021/am501002z | ACS Appl. Mater. Interfaces 2014, 6, 7712−7718

ohmic resistance of the membrane, and A is the cross-sectional area of the material.

RESULTS AND DISCUSSION

Preparation and Structure of Pressed Membranes. In order to prepare the pressed silica colloidal membranes, we generated Stöber silica spheres and calcinated them at 600 °C for 4 h. Calcination is commonly used to prevent crack formation in large-area silica colloidal crystals.[31] Calcination removes water and ethanol that become trapped inside the silica spheres during their formation. As the result of the calcination, silica spheres shrink and increase their density (ca. 2.17 g/cm^3 compared to ca. 1.97 g/cm^3 for as-made silica spheres).[31]

Calcinated silica spheres were pressed and sintered at 1050 °C, as described in the Materials and Methods section. The resulting membranes (Figure 2) are robust and durable, having

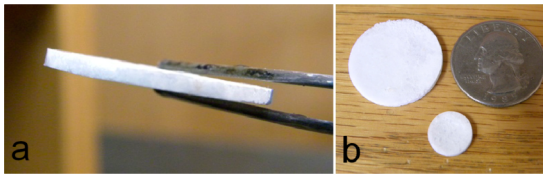

Figure 2. Left: side view of pressed sinteres silica colloidal membrane 25 mm in diameter and ~1 mm in thickness. Right: front view of 25- and 11 mm-diameter membranes in comparison with a ¢25 coin.

uniform thickness and fixed circular shape. For ca. 1 mm thick membranes, the thickness in different spots of the membrane was uniform within the digital calipers resolution (0.01 mm). The uniform thickness of the membranes results from pressing in a die set, where the pressure is distributed evenly. The overall thickness is precisely controlled by the amount of the silica spheres loaded into the die set. In contrast, membranes prepared via vertical deposition are usually thinner at the top of the membrane (the side that was on top of the support during the vertical deposition process) and thicker at the bottom by as much as a factor of 2. This problem is common for vertical deposition preparation and arises from sedimentation of silica spheres during the solvent evaporation in vertical deposition process.

The membranes could be manipulated, sonicated, sandwiched between plastic or metal gaskets, and even dropped from a 1 m height without breaking or cracking. Optical microscopy at 50× magnification (Figure 3) showed minor cracks on the surface of the membranes, which are not seen at the 200× magnification or to the naked eye (Figure 3). However, as will be discussed below, based on the diffusion measurements we concluded that the cracks do not penetrate the entire thickness of the membrane.

We tested the flexural strength of silica colloidal membranes using the apparatus described above, and found it to be 19 ± 6 MPa (2700 ± 800 psi). This value is ca. 17% of the flexural strength of acrylic (17,000 psi) and is about 40% of flexural strength of ordered silica colloidal membranes prepared by vertical deposition (49 ± 9 MPa, 7000 ± 1200 psi). The latter result is expected as ordered silica colloidal membranes contain a close-packed arrangement with the maximum number of contacts between the silica spheres, while pressed membranes are disordered with silica spheres having fewer contacts with

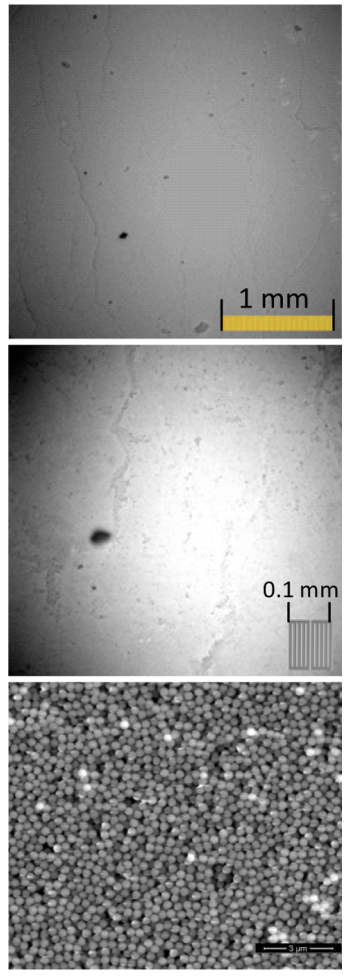

Figure 3. Images of pressed and sintered membrane composed of 390 nm silica spheres. Top: optical microscopy image with 50× magnification. Middle: optical microscopy image with 200× magnification. Bottom: SEM image, scale bar is 3 μm.

their neighbors, i.e. fewer connection points after sintering, which reduces the mechanical strength of the membrane.

This disordered structure can be seen in the SEM image of the pressed membrane (Figure 3). The SEM images of pressed membranes show no visible long- or short-range order of silica particles in the assembly, thus nanopore size cannot be established from silica sphere diameter, unlike in ordered silica colloidal crystal membranes, where nanopore size can be calculated using simple geometrical considerations.[32] For example, because the molecular transport through such ordered membranes occurs normal to the (111) plane of the fcc-packed structure and diffusing species enter the membrane through the concave triangular openings between the adjacent silica spheres, the "radius" of the pores can be defined as the distance from the center of their projection to the nearest sphere surface, which is ca. 15% of the sphere radius. In contrast, for pressed colloidal membranes the voids in several locations in SEM image appear to be larger than the silica sphere diameter.

To further characterize the geometry of pressed silica colloidal membranes, we studied the diffusion of the generation-1 dye-labeled PAMAM dendrimer[25] through the membrane composed of silica spheres 390 nm in diameter. We measured the diffusion rate R_D through the membrane of a known thickness L and area S driven by a known concentration

gradient ΔC. R_D was found by measuring the number of moles of the dendrimer that diffused through the membrane as a function of time. Knowing the value of R_D allowed to calculate the molecular flux J_{membr} through the membrane:

$$R_D = J_{membr} \times S \quad (1)$$

A solution of Fick's law for diffusion

$$J_{membr} = \frac{\Delta C}{L} \times D_{membr} \quad (2)$$

was then used to calculate the diffusion coefficient D_{membr} of a diffusing dendrimer species as it traversed the pressed silica colloidal membrane.

We found the diffusion coefficient of $1.4 \pm 0.4 \times 10^{-10}$ m^2/s for the dendrimer. This value is 2.7 times smaller than the diffusion coefficient of this dendrimer in solution ($3.8 \pm 0.1 \times 10^{-10}$ m^2/s) determined by diffusion NMR.[33] This D_{membr} value reflects the effect of the membrane geometry described by void fraction (ε) and tortuosity (τ) and related to the diffusion coefficient in solution D_{sol} as follows:

$$D_{membr} = \frac{\varepsilon}{\tau} \times D_{sol} \quad (3)$$

Therefore, a smaller D_{membr} for pressed membranes compared to D_{sol} results from the void fraction for the membrane that is less than unity and its tortuosity that may be more than unity. For the ordered closed-packed colloidal crystal the void fraction ε_{fcc} is 0.26 and the tortuousity τ_{fcc} is 3.0, reducing the D_{fcc} by the factor of 11.5 compared to D_{sol}. In contrast, D_{membr} for the disordered pressed colloidal membrane is only 2.7 smaller than D_{sol}, which suggests the void fraction is larger than 0.26 and tortuosity is smaller than 3.0. Because both values affect D_{membr}, it is impossible to calculate them using this value alone. Thus, we calculated the void fraction of the pressed membrane independently, based on its volume displacement. Assuming the pressed silica membrane to be a perfect cylinder of known diameter and thickness, we calculated the total volume of the membrane. Using the weight of the membrane and density of silica (2.17 g/cm^3) and of air inside the membrane (1.20×10^{-3} g/cm^3), we then calculated the void fraction of the membrane. We estimated ε_{membr} to be 0.37, significantly higher than 0.26 of the fcc-packed colloidal crystals. Based on this value and D_{membr}, tortuousity τ_{membr} of the pressed membrane is 1.0. In other words, the transport through the pressed colloidal membranes proceeds in a linear path as opposed to the fcc-packed colloidal crystals.

Size-Exclusion in Pressed Silica Colloidal Membranes. In order to determine the size cutoff for the transport through pressed colloidal membranes, and to establish if the cutoff can be controlled by varying the silica spheres diameter, we measured the diffusion of polystyrene spheres through the pressed membranes composed of silica spheres with different sizes. A representative plot of the flux for polystyrene (PS) spheres 25, 100, and 250 nm in diameter through the pressed membrane composed of 390 nm silica spheres (membrane-390) is shown in Figure 4A. Polystyrene spheres of all three sizes diffuse through the pressed membrane. The flux of 25 nm PS spheres is ca. 10 times greater than that for 250 nm PS spheres and ca. 4 times greater than that of 100 nm PS, which results from both the membrane geometry and the difference in solution diffusion coefficients of the PS spheres. The fact that all PS particles diffuse through this membrane indicates that membrane-390 possesses the size cutoff greater than 250 nm.

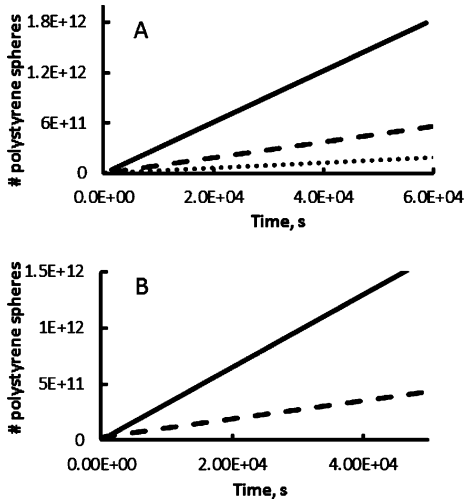

Figure 4. Representative flux plots of PS particles (25 nm PS (−), 100 nm PS (- -), 250 nm PS (···)) through pressed silica colloidal membranes composed of (A) 390 nm silica spheres and (B) 220 nm silica spheres.

This is more than a half of the diameter of the silica spheres used to prepare the membrane. In contrast, ordered silica colloidal crystals, which possess uniform pores with pore "diameter" of ∼15% of silica sphere diameter,[25] would provide a size cutoff of 59 nm in the case of 390 silica spheres.

Next, we tested the cutoff of pressed silica membranes made of 220 and 70 nm silica spheres (membrane-220 and membrane-70, respectively). The plot of the flux of PS spheres through membrane-220 is shown in Figure 4B. No significant diffusion of 250 nm PS spheres through this membrane was observed, thus 220 nm silica spheres upon pressing form colloidal membranes with cutoff of at least 250 nm. However, membrane-220 was permeable for both 25 and 100 nm PS spheres. The flux of 25 nm PS spheres through the membrane-220 is ca. 5 times greater than the flux of 100 nm PS spheres. Taking into account the difference between solution diffusion coefficients D_{sol} of 25 nm PS and 100 nm PS (inversely proportional to the hydrodynamic particle diameter), the diffusion coefficient D_{membr} of 25 nm PS through membrane-220 is ca. 25% greater compared to 100 nm PS. The flux of 25 nm PS through membrane-220 is almost the same as that through membrane-390. The flux of 100 nm PS spheres through membrane-220 is about 2.5 times smaller than that for membrane-390. Membrane-70 is also not permeable for 250 nm PS spheres but permeable for 25 and 100 nm PS beads (data not shown). The flux of 25 nm PS through membrane-70 is 20% greater than that for 100 nm PS, presumably due to sterics rather than diffusion coefficients of PS spheres. Both values are smaller than those for membrane-220 by the factor of ca. 7 and 1.5, respectively. Based on these observations, we conclude that the cutoff for membrane-70 is greater than 100 nm; however, there is a smaller number of larger pores available than in the other two membranes. The observed selectivity of membrane-70, which is lower than expected, can be rationalized in terms of the silica sphere packing that deviates significantly from the close-packed arrangement.

Thus, pore size in pressed membranes could be larger than actual silica sphere size; however, the average pore size still depends on silica sphere size and can be controlled by varying the diameter of the silica particles. Pressed membranes can

block the diffusion of certain particles if small silica spheres are used for the preparation of the membranes.

Pore-Filling of Pressed Silica Colloidal Membranes. In order to further demonstrate the utility of pressed colloidal membranes, we filled their pores with sulfonated polymer brushes formed by surface-initiated atom transfer radical polymerization (ATRP) and measured the proton conductivity of the resulting pore-filled materials. In this case, the sintered assembly of silica colloidal spheres provided the mechanically stable scaffold with interconnected nanopores, suitable for the preparation of fuel cell membranes.

Sintered silica colloidal membranes were rehydroxylated in the presence of a base in order to restore the surface hydroxyl groups. The membrane surface was then aminated followed by ATRP initiator 2-bromo-isobutyryl bromide. Brushes of poly(3-sulfopropyl methacrylate), PSPM, were grown on the silica surface inside the membrane mesopores via surface-initiated ATRP of 3-sulfopropyl methacrylate (Scheme 1). Pore-filled membranes were characterized using thermogravimetric analysis (TGA) and scanning electron microscopy (SEM).

Scheme 1. Preparation of PSPM Brushes

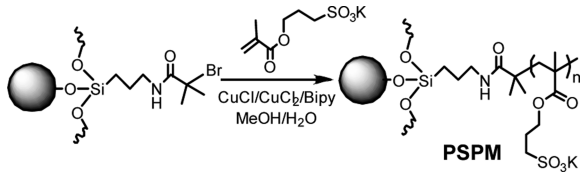

SEM images (Figure 5) confirmed that filling the colloidal mesopores with the polymer brushes does not alter the

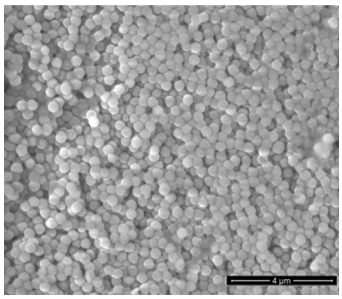

Figure 5. SEM image of a pressed sintered silica colloidal membrane pore-filled with poly(3-sulfopropyl methacrylate) brushes. Scale bar = 4 μm.

integrity of the membrane. The TGA weight loss for PSPM-filled silica colloidal membrane was ca. 4%, which corresponds to ca. 8 nm dry or ca. 60 nm swollen polymer brush, estimated as described earlier.[30] In close-packed ordered silica colloidal crystals containing face-centered cubic arrangements of silica spheres, the distance from the center of the tetrahedral voids, which form the mesopores, to the nearest silica sphere surface is 22.5% of the sphere radius (calculated by elementary trigonometry). For a close-packed membrane composed of 390 nm diameter silica spheres this distance is of 44 nm. The pressed membranes have a larger void fraction with larger average pore dimension. However, since the conductivity measurements were carried out at 98% RH, we assume that polymer brushes were fully hydrated and swollen and thus filled the colloidal mesopores completely. These results are similar to those obtained earlier for ordered silica colloidal membranes pore-filled with PSPM[30] and with PAAM,[32] PNIPAM[34] and PDMAEMA,[35] for all of which the complete pore-filling has been demonstrated.

The proton conductivity obtained for the PSPM-filled pressed membrane at room temperature and 98% R.H. was 0.011 ± 0.007 S/cm, which is high and comparable to that of Nafion reported in the literature[36] and measured using our experimental setup (0.010 ± 0.004 S cm^{-1}). It is also similar to the proton conductivity measured by us for ordered silica colloidal membranes pore-filled with PSPM, which was ~0.02 S/cm at 30 °C and 94% R.H.[30]

CONCLUSIONS

We demonstrated that robust nanoporous membranes with uniform thickness can be prepared by pressing calcinated silica spheres followed by sintering at 1050 °C. The diameter and thickness of the pressed membranes can be controlled by the size of the die set and the loading of the silica spheres, respectively. The pressing/sintering is one of the fastest, easiest, and most reliable processes for the preparation of inorganic nanoporous membranes both on the lab scale and potentially in large-scale manufacturing, it allows time-, cost-, and material-efficient preparation without using solvents, catalysts, or additional reagents. These characteristics compare favorably to commercially available inorganic membranes, such as zeolite membranes and anodized alumina. The former can be prepared with controlled area and thickness, uniform pores and thermal and mechanical stability. However, the zeolite membrane fabrication process is usually involved and slow as it uses one of the following methods: secondary growth on seeded supports, crystallization by microwave heating, stacking of silica nano-blocks, and oriented growth.[37] In addition, they possess small pores with narrow size range and have to be supported. Inorganic nanoporous membranes prepared using aluminum anodization[38,39] provide tunable porosity and are free-standing but require specialized preparation techniques and are quite expensive.

The sphere arrangement in pressed/sintered colloidal membranes is disordered, and their pore size is not uniform. They are capable of size-selective separations, as shown by diffusion experiments for polystyrene spheres of different size. For example, 250 nm polystyrene spheres did not diffuse through the pressed membranes composed of 220 and 70 nm silica spheres, while 100 nm polystyrene spheres showed very small flux through the latter. The size selectivity is not as high as that found for ordered colloidal membranes prepared by vertical deposition but could be useful in separating particles of significantly different sizes. A brief comparison of pressed membranes with vertically deposited membranes is given in Table 1.

We believe that the main utility of pressed/sintered colloidal membranes is in the area of porous inorganic matrices for ion conducting and other functional materials. Indeed, we demonstrated that pressed silica colloidal membranes can be used as a scaffold for the preparation of pore-filled fuel cell membranes. We filled the pores with sulfonated polymer brushes and measured the proton conductivity of the material, which was high and comparable to that of Nafion, thus showing that pore-filled pressed/sintered colloidal membranes may be suitable for applications in fuel cells.

Our present work on pressed/sintered colloidal membranes includes the modification of the silica surface inside the membrane with organic moieties and polymer brushes to

Table 1. Comparison of Silica Colloidal Membranes Prepared by Vertical Deposition and by Pressing of Silica Spheres

	membrane prepared by	
characteristic	vertical deposition	pressing/sintering
controlled thickness	no	yes
controlled area	no	yes
size-selectivity	high	moderate
pore filling	yes	yes
porosity, %	26	37
tortuosity	3	1
preparation time, h	72	12

improve size selectivity and introduce other modes of selectivity. Size- and charge-selective separations of biomacromolecules using pressed silica colloidal membranes are being studied as well.

AUTHOR INFORMATION

Corresponding Author

*E-mail: i.zharov@utah.edu.

Notes

The authors declare no competing financial interest.

ACKNOWLEDGMENTS

This work was supported by the National Science Foundation (CHE-1213628 and DMR-1121252). The authors thank Mr. Matthew Streeter (University of Utah) for his help in constructing the 4-point flexural strength testing apparatus.

REFERENCES

(1) Gin, D. L.; Noble, R. D. Designing the Next Generation of Chemical Separation Membranes. *Science* **2011**, *332*, 674−676.

(2) Hotta, K.; Yamaguchi, A.; Teramae, N. Deposition of Polyelectrolyte Multilayer Film on a Nanoporous Alumina Membrane for Stable Label-Free Optical Biosensing. *J. Phys. Chem. C* **2012**, *116*, 23533−23539.

(3) Deng, J.; Toh, C.-S. Impedimetric DNA Biosensor Based on a Nanoporous Alumina Membrane for the Detection of the Specific Oligonucleotide Sequence of Dengue Virus. *Sensors* **2013**, *13*, 7774−7785.

(4) Tong, H. D.; Jansen, H. V.; Gadgil, V. J.; Bostan, C. G.; Berenschot, C. G. E.; van Rijn, C. J. M.; Elwenspoek, M. Silicon Nitride Nanosieve Membrane. *Nano Lett.* **2004**, *4*, 283−287.

(5) Toh, C.-S.; Kayes, B. M.; Nemanick, E. J.; Lewis, N. S. Fabrication of Free-Standing Nanoscale Alumina Membranes with Controllable Pore Aspect Ratios. *Nano Lett.* **2004**, *4*, 767−770.

(6) Yoshida, M.; Asano, M.; Suwa, T.; Reber, N.; Spohr, R.; Katakai, R. Creation of Thermo-responsive Ion-track Membranes. *Adv. Mater.* **1997**, *9*, 757−758.

(7) Liu, N. G.; Dunphy, D. R.; Atanassov, P.; Bunge, S. D.; Chen, Z.; Lopez, G. P.; Boyle, T. J.; Brinker, C. J. Photoregulation of Mass Transport through a Photoresponsive Azobenzene-Modified Nanoporous Membrane. *Nano Lett.* **2004**, *4*, 551−554.

(8) Nunes, S. P.; Behzad, A. R.; Peinemann, K.-V. Self-Assembled Block Copolymer Membranes: From Basic Research to Large-Scale Manufacturing. *J. Mater. Res.* **2013**, *28*, 2661−2665.

(9) Kato, T.; Yasuda, T.; Kamikawa, Y.; Yoshio, M. Self-Assembly of Functional Columnar Liquid Crystals. *Chem.Commun.* **2009**, *7*, 729−739.

(10) Gin, D. L.; Bara, J. E.; Noble, R. D.; Elliott, B. J. Polymerized Lyotropic Liquid Crystal Assemblies for Membrane Applications. *Macromol. Rapid Commun.* **2008**, *29*, 367−389.

(11) Kato, T.; Mizoshita, N.; Kishimoto, K. Functional Liquid-Crystalline Assemblies: Self-Organized Soft Materials. *Angew. Chem., Int. Ed.* **2006**, *45*, 38−68.

(12) Sakka, S. *Handbook of Sol-Gel Science and Technology*; Kluwer Academic Publishers: Norwell, MA, 2005.

(13) Gestel, T. V.; Hauler, F.; Bram, M.; Meulenberg, W. A.; Buchkremer, H. P. Synthesis and Characterization of Hydrogen-Selective Sol-Gel SiO_2 Membranes Supported on Ceramic and Stainless Steel Supports. *Sep. Purif. Technol.* **2014**, *121*, 20−29.

(14) Park, J.; Jung, M. Hydrogen Permeation of SiC-CeO_2 Composite Membrane by Dip-coating Process. *J. Korean Ceram. Soc.* **2013**, *50*, 485−488.

(15) Miyajima, K.; Eda, T.; Nair, B. N.; Honda, S.; Iwamoto, Y. Hydrothermal Stability of Hydrogen Permselective Amorphous Silica Membrane Synthesized by Counter Diffusion Chemical Vapor Deposition Method. *J. Ceram. Soc. Jpn.* **2013**, *121*, 992−998.

(16) Xu, H.; Goedel, W. A. From Particle-Assisted Wetting to Thin Free-Standing Porous Membranes. *Angew. Chem., Int. Ed.* **2003**, *42*, 4694−4696.

(17) Xu, H.; Goedel, W. A. Polymer-Silica Hybrid Monolayers as Precursors for Ultrathin Free-Standing Porous Membranes. *Langmuir* **2002**, *18*, 2363−2367.

(18) Stroeve, P.; Ileri, N. Biotechnical and Other Applications of Nanoporous Membranes. *Trends Biotechnol.* **2011**, *29*, 259−266.

(19) Kanezashi, M.; Sasaki, T.; Tawarayama, H.; Yoshioka, T.; Tsuru, T. Hydrogen Permeation Properties and Hydrothermal Stability of Sol-Gel-Derived Amorphous Silica Membranes Fabricated at High Temperatures. *J. Am. Ceram. Soc.* **2013**, *96*, 2950−2957.

(20) Ghosh, D.; Sinha, M. K.; Purkait, M. K. A Comparative Analysis of Low-Cost Ceramic Membrane Preparation for Effective Fluoride Removal Using Hybrid Technique. *Desalination* **2013**, *327*, 2−13.

(21) Zhu, Y.; Chen, S.; Quan, X.; Zhang, Y.; Gao, C.; Feng, Y. Hierarchical Porous Ceramic Membrane with Energetic Ozonation Capability for Enhancing Water Treatment. *J. Membr. Sci.* **2013**, *431*, 197−204.

(22) Jiang, H.; Meng, L.; Chen, R.; Jin, W.; Xing, W.; Xu, N. Progress on Porous Ceramic Membrane Reactors for Heterogeneous Catalysis over Ultrafine and Nano-sized Catalysts. *Chin. J. Chem. Eng.* **2013**, *21*, 205−215.

(23) Wong, S.; Kitaev, V.; Ozin, G. A. Colloidal Crystal Films: Advances in Universality and Perfection. *J. Am. Chem. Soc.* **2003**, *125*, 15589−15598.

(24) Bohaty, A. K.; Smith, J. J.; Zharov, I. Free-Standing Silica Colloidal Nanoporous Membranes. *Langmuir* **2009**, *25*, 3096−3101.

(25) Ignacio-de Leon, P. A.; Zharov, I. Size-Selective Transport in Colloidal Nano-Frits. *Chem. Commun.* **2011**, *47*, 553−555.

(26) Zharov, I.; Khabibullin, A. Surface-Modified Silica Colloidal Crystals: Nanoporous Materials with Controlled Molecular Transport. *Acc. Chem. Res.* **2014**, *47*, 440−449.

(27) Birnbaum, A. J.; Zalalutdinov, M. K.; Wahl, K. J.; Pique, A. Fabrication and Response of Laser-Printed Cavity-Sealing Membranes. *J. Microelectromech. Syst.* **2011**, *20*, 436−440.

(28) Stöber, W.; Fink, A.; Bohn, E. Controlled Growth of Monodispersed Spheres in the Micron Size Range. *J. Colloid Interface Sci.* **1968**, *26*, 62−69.

(29) Hiramatsu, H.; Osterloh, F. pH-Controlled Assembly and Disassembly of Electrostatically Linked CdSe-SiO_2 and Au-SiO_2 Nanoparticle Clusters. *Langmuir* **2003**, *19*, 7003−7011.

(30) Smith, J. J.; Zharov, I. Preparation and Proton Conductivity of Self-Assembled Sulfonated Polymer-Modified Silica Colloidal Crystals. *Chem. Mater.* **2009**, *21*, 2013−2019.

(31) Chabanov, A. A.; Jun, Y.; Norris, D. Avoiding Cracks in Self-Assembled Photonic Band-Gap Crystals. *J. Appl. Phys. Lett.* **2004**, *84*, 3573−3575.

(32) Schepelina, O.; Zharov, I. Polymer-Modified Opal Nanopores. *Langmuir* **2006**, *22*, 10523−10527.

(33) Fritzinger, B.; Scheler, U. Scaling Behaviour of PAMAM Dendrimers Determined by Diffusion NMR. *Macromol. Chem. Phys.* **2005**, *206*, 1288−1291.

(34) Schepelina, O.; Zharov, I. PNIPAAM-Modified Nanoporous Colloidal Films with Positive and Negative Temperature Gating. *Langmuir* **2007**, *23*, 12704−12709.
(35) Schepelina, O.; Poth, N.; Zharov, I. pH-Responsive Nanoporous Silica Colloidal Membranes. *Adv. Funct. Mater.* **2010**, *20*, 1962−1969.
(36) Zhang, X. J. Porous Organic-Inorganic Hybrid Electrolytes for High-Temperature Proton Exchange Membrane Fuel Cells. *J. Electrochem. Soc.* **2007**, *154*, B322−B326.
(37) Caro, J.; Noack, M. Zeolite Membranes - Recent Developments and Progress. *Microporous Mesoporous Mater.* **2008**, *115*, 215−233.
(38) Diggle, J. W.; Downie, T. C.; Goulding, C. W. Anodic Oxide Films on Aluminum. *Chem. Rev.* **1969**, *69*, 365−405.
(39) Poinern, G. E. J.; Ali, N.; Fawcett, D. Progress in Nano-Engineered Anodic Aluminum Oxide Membrane Development. *Materials* **2011**, *4*, 487−526.